A second distinct structural "state" of high-density amorphous ice at 77 K and 1 bar

Thomas Loerting, Christoph Salzmann, Ingrid Kohl, Erwin Mayer and Andreas Hallbrucker*

Institut für Allgemeine, Anorganische und Theoretische Chemie, Universität Innsbruck, A-6020 Innsbruck, Austria. E-mail: andreas.hallbrucker@uibk.ac.at

High-density amorphous ice (HDA), further densified on isobaric heating from 77 K to 165 (177) K at 1.1 (1.9) GPa, relaxes at 77 K and 1 bar to the same structural "state" with a density of 1.25 ± 0.01 g cm^{-3}. Its density is higher by ≈ 9% than that of HDA, and thus it is called very-high-density amorphous ice (VHDA). X-ray diffractogram and Raman spectrum of VHDA clearly differs from that of HDA, and the hydrogen-bonded O–O distance increases from 2.82 Å in HDA to 2.85 Å in VHDA. Implications for the polyamorphism of the amorphous forms of water are discussed.

Introduction

A high-density amorphous form of ice (HDA) made by compression of hexagonal ice (ice Ih) at 77 K and 1.0 GPa was reported by Mishima et al.[1,2] We find that after isobaric heating of this HDA at pressures of either 1.1 or 1.9 GPa from 77 K up to 165 or 177 K, a second distinct structural form of high-density amorphous ice can be recovered at 77 K and 1 bar. It was characterized by X-ray diffraction, density measurements and Raman spectroscopy. It is denser than HDA and converts back toward HDA on isochoric heating to 140 K at a starting pressure of 0.02 GPa. Our observation of a second distinct structural "state" of high-density amorphous ice at 77 K and 1 bar is important for our understanding of disordered systems and the transitions between these.

Results and discussion

We first prepared HDA by compression of ice Ih at 77 K up to 1.2 GPa in a commercially available piston-cylinder apparatus with 8 mm diameter piston (Specac Company), by using a computerized "universal testing machine" (Zwick, Model BZ100/TL3S) for compression at a controlled rate of 7000 N min^{-1}. Its positional reproducibility is ±5 μm, and the spatial resolution of the drive is 0.01 μm. Pressure–displacement curves were recorded with the TestXpert V 7.1 Software of Zwick. Indium linings were used as decribed in ref. 3 to avoid pressure drops during compression, and 0.250 cm^3 of water were pipetted into the precooled piston-cylinder apparatus.

Fig. 1A shows the change in volume, ΔV, on compression of ice Ih at 77 K up to 1.2 GPa (marked as a′). ΔV values were calculated from the displacement by assuming that the diameter of the piston remains constant. This curve has the same shape as pressure–displacement curves reported e.g. by Mishima et al.,[1,2] and as that shown in Fig. 1a of ref. 3. The pronounced decrease in volume on compression above ≈ 1.1 GPa is due to the phase transition of ice Ih to HDA. The

transformation begins at slightly higher pressure than reported before[1,2,4–9] which is attributed to friction in the piston-cylinder apparatus. These pressure–displacement curves without pressure drops are characteristic for formation of HDA without ice XII.[3] HDA recovered after compression under liquid N_2 at 1 bar was characterized by X-ray diffraction. Its diffractogram, shown in Fig. 1 as curve A′, is that reported in the literature,[1,2,4,5] with the maximum of the intense broad peak at 3.0 Å. The pressures given in the following are nominal pressures, and the pressures at the sample are expected to be slightly lower. Temperature was measured with a thermocouple firmly attached to the outside of the piston cylinder apparatus, and the accuracy is estimated as ±2 K by following the glass–liquid transition of glycerol at ambient pressure. Heating rate was ≈ 6 K min^{-1} at 110 K, and it decreased linearly to ≈ 4 K min^{-1} at 165 K. The Raman spectrum of HDA containing 5 wt.% D_2O is shown in Fig. 2 (middle), and peak positions of the coupled OH and decoupled OD stretching bands are consistent with those reported in the literature.[10–12] The translational HDA band centered at ≈ 205 cm^{-1} (Fig. 2, right) compares well with that reported by Suzuki et al.[13] for annealed HDA at about 200 cm^{-1} whereas Kanno et al.[12] had reported a lower HDA peak frequency of 180 cm^{-1}. The broad band at higher frequency, attributable to a librational mode, is similar to that shown by Kanno et al. in their Fig. 2.[12]

HDA gradually densifies further on heating at a constant pressure of 1.1 GPa up to ≈ 165 K (Fig. 1B). The pronounced ΔV change on heating from ≈ 80 to 90 K corresponds to the region where liquid N_2 had evaporated and slow warming of the apparatus begins. At the temperature of ≈ 165 K marked as b′ the sample was cooled to liquid N_2 and recovered under liquid N_2 at 1 bar. Thereafter it was characterized either by its X-ray diffractogram (shown in Fig. 1 as curve B′) or by its Raman spectrum (Fig. 2, top). The X-ray diffractogram of the recovered sample shows pronounced differences to that of HDA: the peak position shifts from 3.0 Å in HDA to 2.75 Å, and the full width at half height (FWHH) decreases. This form of recovered high-density amorphous ice is called VHDA (for "very-high density amorphous ice") in order to differentiate from HDA. The Raman spectrum of recovered VHDA (Fig. 2, top) also clearly differs from that of HDA in that the peak position of the decoupled OD stretching transition is shifted by 20 cm^{-1} to higher frequency and that of the coupled OH stretching transition by ≈ 30 cm^{-1}. The translational HDA band centered at ≈ 205 cm^{-1} shifts to ≈ 190 cm^{-1} in VHDA (Fig. 2, right). Our observation of the pronounced shift of the peak maximum in the X-ray diffractogram (Fig. 1, curve A′ versus B′) is consistent with Mishima's report that HDA ices heated or annealed to 130–150 K at 1.0–1.5 GPa "show identical X-ray patterns (with a halo peak around 2.75 Å)".[5]
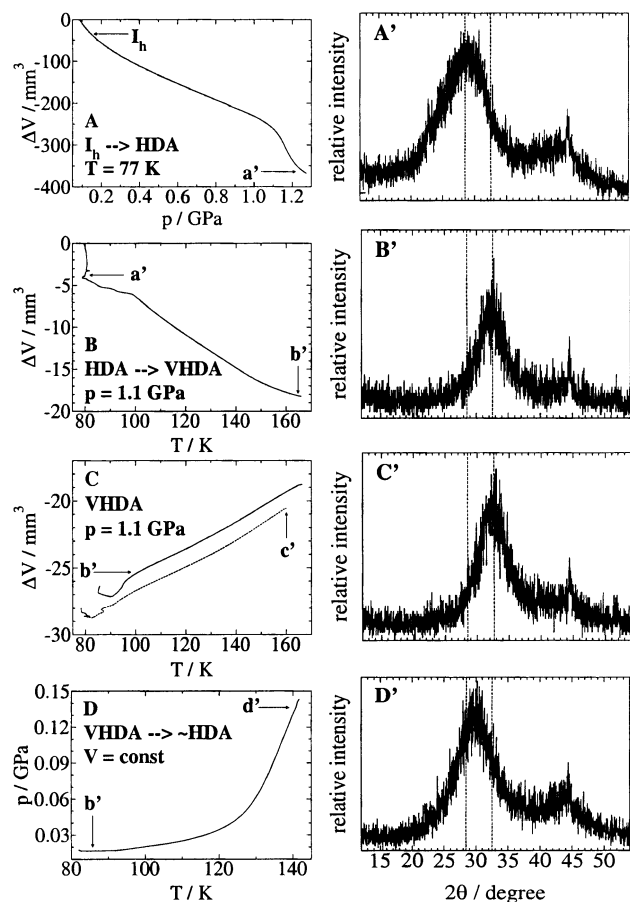
Fig. 1 Conversion of HDA to VHDA and back to HDA as shown by ΔV versus T(or p) plots (A to D) and X-ray patterns (A′ to D′). (A) The ΔV versus p plot shows the conversion of ice Ih to HDA on compression at 77 K up to 1.2 GPa (marked by a′), and (A′) the X-ray pattern of HDA recovered at 77 K and 1 bar. In plots B to D arrows and small letters indicate the temperatures where in subsequent experiments the material was characterized by heating up to the temperature, cooling thereafter under pressure to liquid N_2, recovering the sample at 1 bar under liquid N_2 and characterizing the sample by X-ray diffraction (plots B′ to D′) or Raman spectroscopy (see Fig. 2). (B) The ΔV versus T plot on isobaric conversion of HDA on heating from 77 K to ≈ 165 K at 1.1 GPa, and (B′) the X-ray pattern of recovered VHDA. (C) The ΔV versus T plot on isobaric cycling of VHDA at 1.1 GPa from 77 to ≈ 165 K (solid: first heating, dotted: second heating), and (C′) the X-ray pattern of recovered VHDA after the two cycles. (D) The p versus T plot on isochoric conversion of VHDA towards HDA with a starting pressure of 0.02 GPa on heating from 77 to ≈ 140 K, and (D′) the X-ray pattern of recovered HDA. The two dotted lines in A′ to D′, and in E′ to G′ of Fig. 3, mark the peak positions of the HDA and VHDA peaks. X-ray diffractograms (Cu-Kα) were recorded on a diffractometer in θ–θ geometry (Siemens, model D 5000), equipped with a low-temperature camera from Paar. The sample plate was in horizontal position during the whole measurement.

We next describe in Figs. 1 and 3 various temperature/pressure treatments of HDA and VHDA, and curves B′, C′ in Fig. 1 and E′, F′ in Fig. 3 are diffractograms with peak position at 2.75 Å characteristic for VHDA.

Densified HDA can be cycled at constant pressure of 1.1 GPa between 80 and ≈ 165 K without reconversion to HDA on pressure release at 77 K. The solid line in Fig. 1C is obtained on first heating, the dotted line on second heating. The two lines are shifted slightly but the slope is identical. VHDA was further characterized after second heating to ≈ 160 K, that is to the temperature marked c′, in the same manner described above, by cooling to 77 K and recording its X-ray diffractogram (curve C′ in Fig. 1). This is indistiguishable from curve B′ obtained on first heating at 1.1
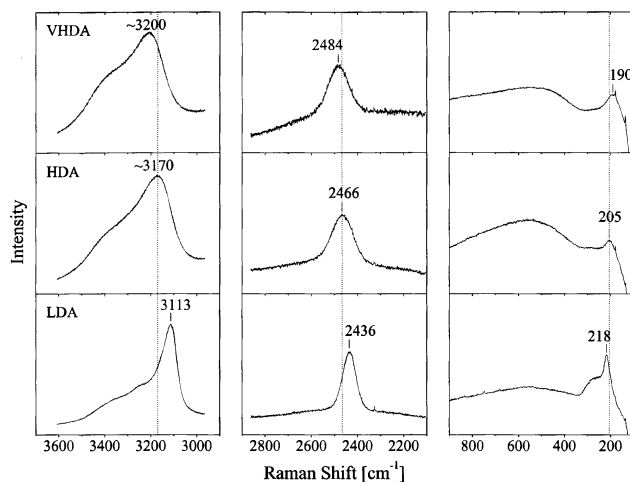

Fig. 2 Raman spectra of HDA and VHDA (containing 5 wt.% D_2O) recovered after compression at 77 K and 1 bar and recorded in vacuo at 80 K. The coupled OH (left), the decoupled OD stretching band region (middle), and the low-frequency region (right) are shown. Middle: HDA made on compression of ice Ih at 77 K; top: VHDA made on heating HDA at 1.1 GPa up to ≈ 165 K; bottom: for comparison LDA made on heating of HDA.
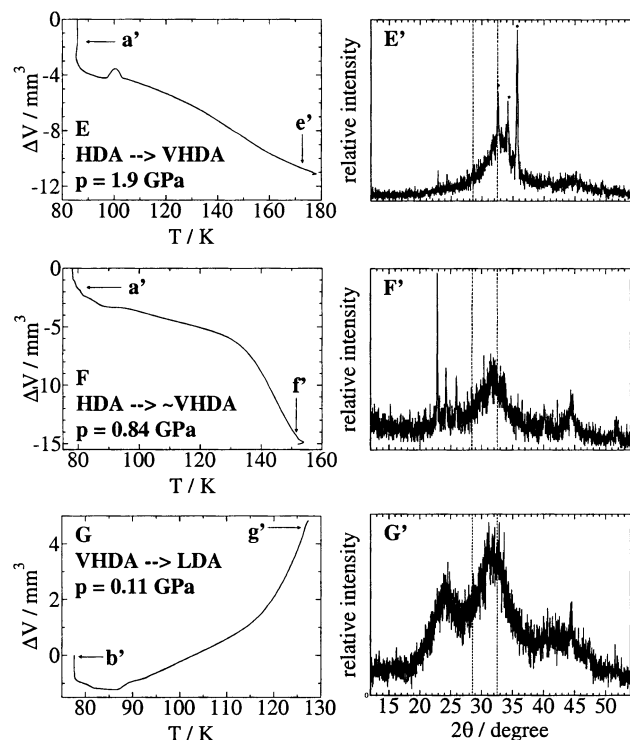

Fig. 3 Conversion of HDA to VHDA on isobaric heating at 1.9 and 0.84 GPa. (E) The ΔV versus T plot on isobaric heating of HDA (a′) at 1.9 GPa from 77 K to ≈ 177 K (e′), and (E′) the X-ray pattern of recovered VHDA. (F) The ΔV versus T plot on isobaric heating of HDA (a′) at 0.84 GPa from 77 K to ≈ 154 K (f′), and (F′) the X-ray pattern of recovered VHDA. (G) The ΔV versus T plot on isobaric heating of VHDA at 0.11 GPa from 77 K (b′) to ≈ 127 K (g′), and (G′) the X-ray diffractogram of the recovered sample from a mixture of VHDA and LDA.

GPa. We further show that VHDA can be converted back toward HDA on isochoric heating to 140 K at a starting pressure of 0.02 GPa (Fig. 1D). After heating to 140 K (marked d′), the sample was cooled to 77 K. The X-ray diffractogram of the recovered sample, shown in Fig. 1 as D′, has a peak maximum close to that of HDA (A′), but its FWHH seems to be slightly less.

HDA was further heated at a constant pressure of 1.9 or 0.84 GPa and the effects controlled by X-ray diffractograms of samples recovered at 77 K and 1 bar (cf. Fig. 3). On isobaric heating of HDA at 1.9 GPa up to 177 K (Fig. 3, curve E) and subsequent cooling to 77 K, the X-ray diffractogram of the recovered sample, shown in Fig. 3 as E′, was indistinguishable from that shown in Fig. 1 as curve B′ or C′. After isobaric heating at 0.84 GPa up to ≈ 155 K (cf. Fig. 3, curve F), the X-ray diffractogram of the recovered sample, shown in Fig. 3 as curve F′, is very similar to that shown as curve E′.

We further show in Fig. 3 that VHDA transforms on heating at a constant pressure of 0.11 GPa directly into low-density amorphous ice (LDA), without HDA being formed in between. Curve G is the ΔV versus T plot recorded on heating VHDA up to 127 K, and curve G′ is the X-ray diffractogram of the recovered sample. The peak maxima of the two broad peaks are at $2\theta \approx 32$ and $\approx 24°$, and thus correspond to VHDA and LDA. HDA as intermediate would have been recognizable by a peak centered at $\approx 29°$.

Densities of VHDA and of HDA were determined at 78 K and 1 bar by flotation in a liquid N_2–Ar mixture, by varying the density of the liquid until the solid remains suspended. The density of the liquid was then determined via buoyancy of a calibrated glass body (with Kern balance model 810/23). Sealed cracks or voids in the samples can change the floating characteristics and give incorrect density values. We have therefore tested the method by determining the densities of recovered ice V and of ice VI which had been made on heating HDA at pressures of 0.5 and 1.6 GPa. Their densities agree within 0.01 g cm^{-3} with those calculated from the X-ray diffraction data and reported in the literature (to be reported separately).[14,15] We are thus confident that the contribution of sealed cracks to the densities of recovered HDA and VHDA can be neglected. We further show below that the HDA and VHDA densities obtained by buoyancy are consistent with those calculated from the volume increase on conversion to low-density amorphous ice (LDA).

The density of VHDA determined by buoyancy is 1.25 ± 0.01 g cm^{-3} (densities were determined after heating at 1.1 GPa as 1.253 and 1.251 g cm^{-3}, and at 1.9 GPa as 1.258 and 1.250 g cm^{-3}), and that of HDA is 1.15 ± 0.01 g cm^{-3} (from batch 1 as 1.146 and 1.150, from batch 2 as 1.153 and 1.150 g cm^{-3}). The HDA value is consistent with that of 1.17 ± 0.02 g cm^{-3} reported by Mishima et al.,[1,2] but not with the HDA value of 1.30 g cm^{-3} reported by Johari.[9] It is conceivable that in the latter case some ice XII had formed on compression of ice Ih at 77 K instead of HDA.[3,16]

Independent estimation of HDA and VHDA densities was obtained via the volume increase on isobaric heating at 0.001 GPa up to 140 K and conversion to LDA. On assuming the LDA density as 0.94 g cm^{-3},[2] the HDA and VHDA densities calculate as 1.14 and 1.26 g cm^{-3} at 77 K and 0.001 GPa.

Mishima et al.[1,2] reported for HDA at 77 K and 1.0 GPa a density of 1.31 ± 0.02 g cm^{-3}. From these values at 77 K (1.15 g cm^{-3} for 1 bar and 1.31 g cm^{-3} for 1.0 GPa) we obtain by linear extrapolation a density estimate of 1.45 (1.33) g cm^{-3} at 1.9 (1.1) GPa. These densities at 77 K allow in turn to estimate the densities at 170 K: in both Fig. 1B and 3E, ΔV becomes increasingly negative with increasing temperature. Thus, the volume decreases and the samples densify on heating. The estimated density at 170 K and 1.1 GPa is ≈ 1.37 g cm^{-3}, and that at 1.9 GPa is ≈ 1.51 g cm^{-3}.

We conclude that HDA, further densified on isobaric heating from 77 K up to 165–177 K at either 1.1 or 1.9 GPa to ≈ 1.37 or ≈ 1.51 g cm^{-3}, relaxes at 77 K and 1 bar to the same structural "state" with a density of 1.25 g cm^{-3}. X-ray diffractograms and Raman spectra of this recovered VHDA clearly differ from those of HDA.

Correlations between the decoupled O–D peak frequency and hydrogen-bonded average O–H $\cdots$ O distance allow to obtain an estimate of O–H $\cdots$ O distances from the Raman spectrum. With the correlation reported in ref. 17 we obtain from the decoupled O–D peak frequencies of Fig. 2 average O–D $\cdots$ O distances of 2.77 Å for LDA, 2.82 Å for HDA and 2.85 Å for VHDA. Thus, on conversion of HDA into VHDA, increasing density is coupled with increasing O–D $\cdots$ O distance, in similar manner to that observed for the LDA → HDA transition.[10] For LDA → HDA this had been attributed entirely to an increase in coordination number,[10] and similar interpretation holds for conversion of HDA into VHDA.

On isobaric heating of HDA either at 1.1 GPa (Fig. 1B) or at 1.9 GPa (Fig. 3E), the volume decreases more or less continuously. Thus, a continuous variety of densities and structural states is formed. This contrasts with our observation that samples recovered at 77 K and 1 bar show the pattern of only one distinct structural form, that is of VHDA. This means that pressurized amorphous ice with a continuous variety of densities up to 1.51 g cm^{-3} (at 170 K and 1.9 GPa) relaxes on release of pressure at 77 K to VHDA with a density of 1.25 g cm^{-3}. This indicates a pronounced minimum in the potential energy megabasin which is distinct from that of HDA formed on compression at 77 K. However, we emphasize that we do not want to imply that HDA and VHDA are related in a manner similar to HDA and LDA,[1,2] and high-density amorphous ice samples with densities in between those of HDA and VHDA at 77 K and 1 bar might be obtainable by other routes.

So far the four amorphous forms of water at 77 K and 1 bar are HDA, LDA, and amorphous water made by deposition of water vapor[18] or by "hyperquenching" of the liquid.[19] VHDA is a fifth structural "state", and it is important for our understanding of polyamorphism and the structure towards which amorphous ice develops with increasing density at constant temperature and pressure.

References

1 O. Mishima, L. D. Calvert and E. Whalley, Nature, 1984, 310, 393.
2 O. Mishima, L. D. Calvert and E. Whalley, Nature, 1985, 314, 76.
3 I. Kohl, E. Mayer and A. Hallbrucker, Phys. Chem. Chem. Phys., 2001, 3, 602.
4 O. Mishima, J. Chem. Phys., 1994, 100, 5910.
5 O. Mishima, Nature, 1996, 384, 546.
6 A. Bizid, L. Bosio, A. Defrain and M. Oumezzine, J. Chem. Phys., 1987, 87, 2225.
7 M. A. Floriano, Y. P. Handa, D. D. Klug and E. Whalley, J. Chem. Phys., 1989, 91, 7187.
8 G. P. Johari, Phys. Chem. Chem. Phys., 2000, 2, 1567.
9 (a) G. P. Johari, J. Chem. Phys., 2000, 112, 8573; (b) G. P. Johari, J. Chem. Phys., 2000, 113, 10412.
10 D. D. Klug, O. Mishima and E. Whalley, J. Chem. Phys., 1987, 86, 5323.
11 E. Whalley, J. Less-Common Met., 1988, 140, 361.
12 H. Kanno, K. Tomikawa and O. Mishima, Chem. Phys. Lett., 1998, 293, 412.
13 Y. Suzuki, Y. Takasaki, Y. Tominaga and O. Mishima, Chem. Phys. Lett., 2000, 319, 81.
14 P. V. Hobbs, Ice Physics, Clarendon Press, 1974.
15 V. F. Petrenko and R. W. Whitworth, Physics of Ice, Oxford University Press, 1999.
16 M. Koza, H. Schober, A. Tölle, F. Fujara and T. Hansen, Nature, 1999, 397, 660.
17 C. A. Tulk, D. D. Klug, R. Branderhorst, P. Sharpe and J. A. Ripmeester, J. Chem. Phys., 1998, 109, 8478.
18 E. F. Burton and W. F. Oliver, Proc. R. Soc. London, Ser. A, 1935, 153, 166.
19 P. Brüggeller and E. Mayer, Nature, 1980, 288, 569.